Simultaneous In Situ Formation of ZnS Nanowires in a Liquid Crystal Template by γ-Irradiation

Xuchuan Jiang, Yi Xie,* Jun Lu, Liying Zhu, Wei He, and Yitai Qian

Structure Research Laboratory and Laboratory of Nanochemistry & Nanomaterials, University of Science & Technology of China, Hefei, Anhui 230026, People's Republic of China

Received July 26, 2000. Revised Manuscript Received February 5, 2001

Semiconductor ZnS nanowires were synthesized by a direct templating route in an inverted hexagonal liquid crystal formed by oligo(ethylene oxide)oleyl ether amphiphiles, *n*-hexane, *n*-hexanol/*i*-propanol (2:1), and water. The final product consists of ordered nanowires with a diameter of ca. 5 nm. Most importantly, seven or more close-packed nanowires aggregate to form a regularly shaped bundle with a width of ca. 10−30 nm, duplicating the hexagonal structure of close-packed inverted micelles formed by amphiphiles. We propose a novel simultaneous in situ formation (SISF) technique to synthesize ordered ZnS nanowires by γ-irradiation at room temperature. The reaction is worth noting in that its occurrence is homogeneous and simultaneous. The structures of the inverted hexagonal liquid crystal phase and the final product were characterized by means of polarized optical microscopy (POM), XRD, XPS, TEM and EDX techniques. UV−vis and PL spectra recorded the optical properties of the ZnS nanowires. The amount of amphiphiles passivated with ZnS nanowires is ∼3.4 wt %, as determined by thermal gravimetric analysis (TGA).

1. Introduction

One-dimensional structures with nanoscale diameters such as nanowires, nanorods, and nanotubes are currently the focus of much attention because of their special properties.[1] Compared to micrometer-diameter whiskers, these fascinating systems are expected to exhibit remarkable mechanical properties, as well as electrical, optical, and magnetical properties that are quite different from those of their corresponding bulk materials.[2] These new nanoscale materials have potential applications in both mesoscopic research and the development of nanodevices. Previous work in this field focused on carbon nanorods and nanotubes, which were the byproducts of fullerene research.[3] Conventionally, carbon nanorods and nanotubes are grown in an arc discharge at a temperature of about 3000 K, by thermal deposition of hydrocarbons, or by vapor−liquid−solid (VLS) growth.[4−6] Comparatively little research has been done on other one-dimensional nanomaterials and, particularly, on the preparation of nanowires, nanorods, or nanotubes at ambient conditions. Recently, Xie and co-workers[7] prepared $CoTe_2$ nanorods and CdSe nanorods[8] via a solvothermal route under mild conditions. Zhang and co-workers[9] synthesized ultrafine bismuth nanowire arrays by injecting a liquid melt into the nanochannels of a porous anodic alumina oxide (AAO) "hard" template. Li and co-workers[10] prepared ordered CdS nanowires in an AAO template as well. It is quite noteworthy that a "soft" liquid crystal phase could directly template a hard mineral phase. The liquid-crystal-template-assisted route to group IIB−VI semiconductor nanowires has received more attention for its special properties, such as convenience in operation and ease in control of morphology. Li[11] also reported the synthesis of parallel nanowires of CdS via a hexagonal liquid crystal soft template. However, Braun and co-workers[12] prepared ZnS, CdS, and CdSe superlattices templated by a hexagonal liquid crystal using H_2S or H_2Se gas rather than semiconductor nanowires.

Like other semiconductor metal chalcogenides, ZnS is a rather interesting material. It has been used as a pigment,[13] in water purification,[14] in electrolumines-

* To whom correspondence should be addressed. E-mail: yxie@ustc.edu.cn.

(1) Rao, A. M.; Richter, E.; Bandow, S.; Chase, B.; Eklund, P. C.; Williams, K. A.; Fang, S.; Subbaswamy, K. R.; Menon, M.; Thess, A.; Smalley, R. E.; Dresselhaus, G.; Dresselhaus, M. S. *Science* **1997**, *275*, 187.

(2) Alivisatos, A. P. *Science* **1996**, *271*, 933.

(3) Iijima, S. *Nature* **1991**, *354*, 56.

(4) Colbert, D. T.; Zhang, J.; McClure, S. M.; Nikolaev, P.; Chen, Z.; Hafner, J. H.; Owens, D. W.; Kotula, P. G.; Carter, C. B.; Weaver, J. H.; Rinzler, A. G.; Smalley, R. E. *Science* **1994**, *266*, 1218.

(5) Ivanov, V.; Nagy, J. B.; Lambin, Ph.; Lucas, A. Zhang, X. B.; Zhang, X. F.; Bernaerts, D.; Van Tendeloo, G.; Amelinckx, S.; Van Landuyt, J. *Chem. Phys. Lett.* **1994**, *223*, 329.

(6) (a) Morales, A. M.; Lieber, C. M. *Science* **1998**, *279*, 208. (b) Duan, X. F.; Lieber, C. M. *Adv. Mater.* **2000**, *12* (2), 298. (c) Wang, N.; Tang, Y. H.; Zhang, Y. F.; Lee, C. S.; Bello, I.; Lee, S. T. *Chem. Phys. Lett.* **1999**, *299* (2), 237.

(7) Xie, Y.; Li, B.; Su, H.; Liu, X.; Qian, Y. *Nanostruct. Mater.* **1999**, *11* (4), 539.

(8) Yu, S.; Wu, Y.; Yang, J.; Han, Z.; Xie, Y.; Qian, Y.; Liu, X. *Chem. Mater.* **1998**, *10*, 2309.

(9) Zhang, Z.; Ying, J. Y.; Dresselhaus, M. S. *J. Mater. Res.* **1998**, *13*, 1745.

(10) Li, Y.; Xu, D.; Zhang, Q.; Chen, D.; Huang, F.; Xu, Y.; Guo, G.; Gu, Z. *Chem. Mater.* **1999**, *11*, 3433.

(11) Li, Y.; Wan, J.; Gu, Z. *Acta Phys.-Chim. Sin.* **1999**, *15*, 1.

(12) (a) Braun, P. V.; Osenar, P.; Stupp, S. I. *Nature* **1996**, *380*, 325. (b) Braun, P. V.; Osenar, P.; Tohver, V.; Kennedy, S. B.; Stupp, S. I. *J. Am. Chem. Soc.* **1999**, *121*, 7302. (c) Braun, P. V.; Stupp, S. I. *Mater. Res. Bull.* **1999**, *34* (3), 463.

(13) Parker, D. H. *Principles of Surface Coating Technology*; Interscience Publishers: New York, 1965, p 79.

(14) Shimoiizaka, J.; Nanjo, M.; Usui, S. *Nippon Kogyo Kaishi* **1972**, *88*, 545.

10.1021/cm0006143 CCC: $20.00
Published on Web 03/23/2001

cence,[15] in nonlinear optical devices,[16] and as an LED when doped.[17] The nanoscale ZnS has a broader energy band gap than its bulk material ($E_g = 3.65$ eV),[18] which extends its application range. Therefore, the synthesis of ZnS nanoparticles and films has been widely investigated in previous work.[19−25] Comparatively, one-dimensional ZnS nanomaterials (nanowires, nanorods, and whiskers) can exhibit special optical and electrical properties compared with semiconductor quantum dots.

In this paper, we report a novel simultaneous in situ formation (SISF) technique for the synthesis of 5 nm × (0.6−1.2 μm) ZnS nanowires via γ-irradiation at room temperature. The so-called SISF technique is based on a mechanism of simultaneous occurrence of the decomposition of thiourea (Tu) or carbon disulfide (CS_2) under γ-irradiation and the formation of ZnS nanowires in an inverted hexagonal liquid crystal phase. It is found that the ZnS nanowires formed are well dispersed before and after removal of the liquid crystal template. In the present work, we adopt thiourea or CS_2 as the sulfur source and avoid the use of toxic H_2S gas. It is much more interesting that the bundle of ZnS nanowires duplicates the structure of the inverted hexagonal liquid crystal phase. Furthermore, we have shown the importance of both the chemical nature and the structure of the amphiphiles in direct templating that opens up a variety of synthetic avenues to the formation of novel nanowires.

2. Experimental Section

Materials. Unless otherwise noted, all reagent-grade chemicals were used as received, and deionized water was used throughout. The amphiphile oligo(ethylene oxide)$_{10}$oleyl ether [(EO)$_{\overline{10}}$oleyl] was obtained from Shanghai Chemical Reagent Ltd. Co. of China. It has an average degree of polymerization of 10 ethylene oxide structural units in its hydrophilic segment and an oleyl hydrophobic segment.

Procedure. In a typical procedure for the preparation of ZnS nanowires, the hexagonal mesophase was formed by mixing 30 vol % (EO)$_{\overline{10}}$oleyl, 30 vol % *n*-hexane, 10 vol % *n*-hexanol/*i*-propanol (2:1), and 30 vol % water. When Zn^{2+} ions were doped, the 30 vol % pure water was substituted with aqueous 0.03 mol dm^{-3} $Zn(NO_3)_2$ solution. Before irradiation with a dose of 1.8×10^4 Gy in the field of a ^{60}Co γ-ray source, an appropriate amount of either aqueous 0.03 mol dm^{-3} thiourea or 0.03 mol dm^{-3} CS_2/*n*-hexane solution was added into the hexagonal liquid crystal system. The ionic doping was controlled and did not disrupt the order of the liquid crystal, similar to the results reported by Braun.[12] After the reaction system was irradiated by γ-ray for 6 h, the resulting metal sulfide−mesophase composite was washed three times to remove byproducts and unbound amphiphiles. Each washing involved dispersing the material in a 50:50 vol % solution of diethyl ether/ethanol via sonication, followed by centrifugation and removal of the clear supernatant. The final product was washed with CS_2 to remove the byproduct of elemental sulfur and then dried in a vacuum at 40 °C for 3 h.

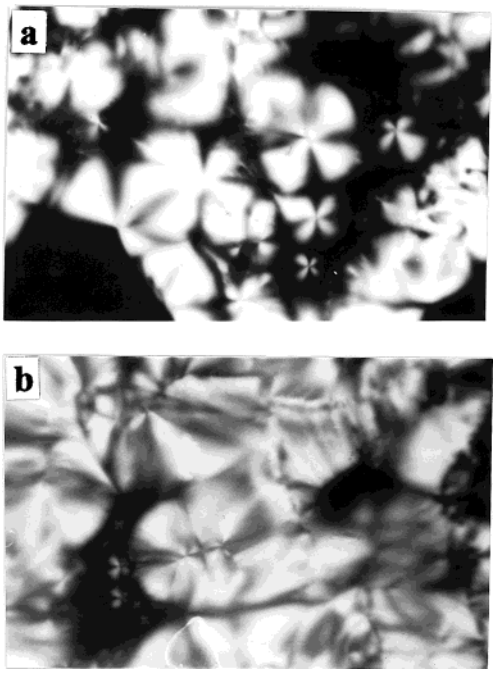

Figure 1. POM patterns of the inverted hexagonal liquid crystal (a) before and (b) after doping with Zn^{2+} ions (×250).

Characterization. The product was characterized as follows. The XRD analysis was carried out with a Rigaku D/max-γ rotating anode X-ray diffractometer, using Ni-filtered Cu K_α radiation ($\lambda = 1.54178$ Å). A scanning rate of 0.05° s^{-1} was applied to record the patterns in the 2θ range of 5−65°. The reflection data were collected at 25 °C. The electronic binding energy of ZnS was examined by X-ray photoelectron spectroscopy (XPS) using an ESCALab MKII instrument with Mg K_α ($h\nu = 1253.6$ eV) radiation as the exciting source and with an energy resolution of 1.0 eV. The binding energy values obtained in the XPS analysis were corrected by referencing the C 1s peak to 284.60 eV. Transmission electron microscopy (TEM) and energy-dispersive X-ray (EDX) analyses were performed with a Hitachi H-800 transmission electron microscope at an acceleration voltage of 200 kV. UV−visible absorption spectra were recorded using an UV−vis spectrophotometer (Specord 200) with a wavelength range of 190−1100 nm (Analytik Jena GmbH, Germany). The photoluminescence (PL) spectrum was recorded using a Hitachi 850 fluorescence spectrophotometer. The amount of amphiphiles bound with ZnS nanowires were determined using a thermal gravimetric analysis instrument (Shimadzu TGA-50H) with a flow rate of 20.0 mL min^{-1} and a heating rate of 10 °C min^{-1}.

3. Results and Discussion

The characteristic average molecular order of the mesophase was not disrupted by the addition of aqueous thiourea or CS_2/*n*-hexane solution. The optical textures observed by polarized optical microscopy (POM) (×250) before and after ionic doping (Figure 1) were similar. As additional proof of order in the mesophase, X-ray diffractograms were collected to characterize both the long periodicity and the symmetry of the mesophase. For a system containing 30 vol % amphiphile, the 100,

(15) Schlam, E. *Proc. IEEE* **1973**, *61*, 894.
(16) Xu. J.; Ji. W. *J. Mater. Sci. Lett*. **1999**, *18*, 115.
(17) Donahue, E. J.; Roxburgh, A.; Yurchenko, M. *Mater. Res. Bull*. **1998**, *33* (2), 323. Sun, L.; Liu, C.; Liao, C.; Yan, C. *J. Mater. Chem*. **1999**, *9* (8), 1655. Papakonstantinou, D. D.; Huang, J.; Lianos, P. *J. Mater. Sci. Lett*. **1998**, *17* (18), 1571. Saenger, D. U.; Jung, G.; Menning, M. *J. Sol−Gel Sci. Technol*. **1998**, *13* (1/3), 635.
(18) Dhas, N. A.; Zaban, A.; Gedanken, A. *Chem. Mater*. **1999**, *11*, 806.
(19) Verna, A. K.; Ranchfuss T. B.; Wilson, S. R. *Inorg. Chem*. **1995**, *34*, 3072.
(20) Dusatre, V.; Omer, B.; Parkin, I. P.; Shaw, G. A. *J. Chem. Soc., Dalton Trans.* **1997**, 3505.
(21) Sugimoto, T.; Chen, S.; Muramatsu, A. *Colloids Surf. A* **1998**, *135*, 207.
(22) Bredol, M.; Merikhi, J. *J. Mater. Sci.* **1998**, *33* (2), 971.
(23) Balaz, P.; Balintova, M.; Bastl, Z.; Briancin, J.; Sepelak, V. *Solid State Ionics* **1997**, *101−103*, 45.
(24) Xu, J.; Ji, W.; Lin, J.; Tang, S.; Du, Y. *Appl. Phys. A: Mater. Sci. Process* **1998**, *A66* (*6*), 639.
(25) Raudel − Tiexier, A.; Leloup, J.; Barraud, A. *Mol. Cryst. Liq. Cryst*. **1986**, *134*, 347.

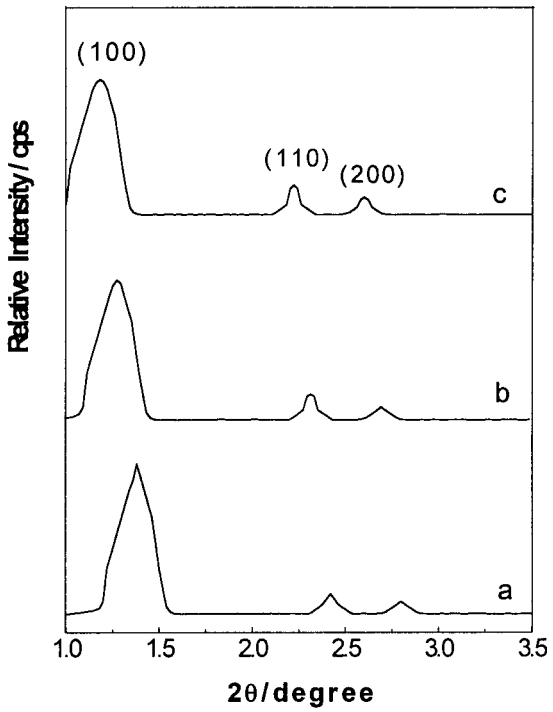

Figure 2. X-ray diffraction patterns of the inverted hexagonal liquid crystal: (a) original phase, (b) after doping with Zn^{2+} ions, and (c) containing final products.

110, and 200 reflection peaks are clearly observed. The inverted hexagonal phase exhibits characteristic diffraction spacings of $1:1/\sqrt{3}:1/\sqrt{4}:...$[26] (Figure 2). Little change was observed in the POM and XRD patterns after doping, which were similar to those previously reported.[12] However, their diffraction patterns and *d* spacings were essentially the same. For successful direct templating, it is important that the liquid crystal phase be stable at all stages of the templating process. For example, when the $(EO)_{\overline{10}}$oleyl-based mesophases were disrupted by doping with 0.2 mol dm^{-3} salt solution, the system separated into two phases, and no expected nanowires were synthesized; therefore, the 0.01−0.1 mol dm^{-3} ZnS solution was substituted for pure water in the formation of the liquid crystal phase.

The templating nature of synthesis within the mesophase was further verified. Braun[12] investigated the relationship between the amphiphile content and the center-to-center distance between cavities or hydrophobic cores in the mineralized structure as measured by TEM or SAXS. The observed correlation between the superlattice dimensions in the precipitate and the lattice constant of the mesophase offers very strong evidence for direct templating. In this case, the ZnS nuclei mineralized in the cavities composed by 30 vol % $(EO)_{\overline{10}}$oleyl liquid crystal phase. On the basis of the assumption that the ZnS is directly templated by the liquid crystal in which it is grown, the hexagonal symmetry and associated periodicity should be nearly identical to that in the precursor of hexagonal mesophase. We obtained the *d* spacings by XRD that were ca. 6.5 nm, corresponding to the 100 reflection (2θ = 1.35°) as shown in Figure 2a. The center-to-center distance between hydrophilic cavities in the precursor mesophases is estimated to be ca. 7.4 nm (Scheme 1). The diameter of each hydrophilic cavity formed by the inverted rodlike micelles is ca. 4.6 nm, according to the literature.[12] The diameter of the ZnS nanowire prepared is ca. 5 nm, with a little increase compared with the diameter of one hydrophilic cavity in the soft template (Scheme 1). The diameters of the ZnS bundles composed by nanowires range from 10 to 30 nm according to TEM images before and after removal of the hexagonal liquid crystal template. These values are consistent with the nature and structure of the original liquid crystal template. The probable process of the formation of ZnS nanowires is shown in Scheme 1.

In the process of simultaneous in situ formation (SISF), γ-irradiation is selected for two reasons: one is that it does not disrupt the texture of the liquid crystal template, as verified by POM and XRD measurements at ambient conditions; the other is that the irradiation energy is so high that the reactants produce some radicals that play an important role in the expected reactions. Li[10] prepared CdS nanowires in a hexagonal liquid crystal template via a flow of H_2S gas at room temperature. Braun[12] prepared ZnS, CdS, and CdSe superlattices templated by hexagonal liquid crystal also under H_2S or H_2Se gas. The gaseous H_2S and H_2Se are toxic and should be carefully used. Here, we used thiourea and CS_2 as sulfur sources. However, thiourea does not react with the zinc salt at room temperature. When the temperature of this hexagonal mesophase was raised to 80 °C (at which point, the texture of hexagonal liquid crystal was partly disrupted), only ZnS particles were obtained. Similarly, CS_2 was added to the hexagonal mesophase and no products were formed at room temperature without γ-irradiation.

In our experiments, the following reactions (eqs 1−5) are likely to be occurring under intense γ-irradiation. The chemical reaction driven by the intense γ-irradiation is to induce water to produce radicals (eq 1). When the concentration of the solution is around 0.01 mol dm^{-3}, the irradiation energy absorbed by the solutes can be ignored. Although the formation mechanism of nanocrystalline sulfides is not entirely clear, it is clear that, as a result of the reduction of the metal ions with solvated electrons produced in solution under γ-irradiation, lower-valence metal ions are formed.[27−29] The Zn^{2+} ions are reduced to Zn^{+} ions by solvated electrons (eq 2).

$$H_2O \xrightarrow{\text{irradiation}} e^-_{aq},\ H_3O^+,\ H^\cdot,\ H_2,\ OH^\cdot,\ H_2O_2 \quad (1)$$

$$Zn^{2+} + e^-_{aq} \rightarrow Zn^{+} \quad (2)$$

Research on γ-irradiation of CS_2 shows the formation of nonionic intermediates, which possibly exist as S radicals[30] (eq 3). The free sulfur radicals are liberated when S radicals are in the solution. The thiourea might form liberated S radicals in the liquid crystal system under γ-irradiation[31] (eq 4). The free S radicals can react with Zn^{+} ions in the hydrophilic cavities of hexagonal

(26) Gray, D. H.; Hu, S.; Juang, E.; Gin, D. L. *Adv. Mater.* **1997**, *9*, 731.

(27) Janes, R.; Stevens, A. D.; Symons, M. C. R. *J. Chem. Soc., Faraday, Trans. 1* **1989**, *85*, 3973.

(28) Moorthy, P. N.; Weiss, J. J. *Nature* **1964**, *201*, 1317.

(29) Qiao, Z.; Xie, Y.; Zhu, Y.; Qian, Y. *J. Mater. Chem.* **1999**, *9*, 1001.

(30) Johnston, F. *J. Phys. Chem.* **1975**, *79*, 419.

Scheme 1. Illustration of the formation process of ZnS nanowires in liquid crystal template

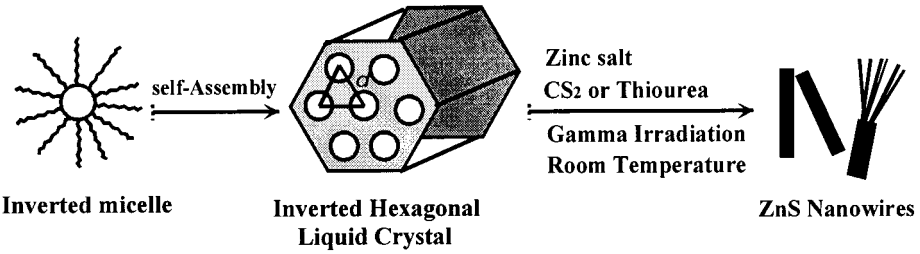

liquid crystal and form ZnS nanocrystallites (eq 5) at room temperature.

$$CS_2 \xrightarrow{\text{irradiation}} S\cdot + CS\cdot \quad (3)$$

$$(NH_2)_2\,CS + 2OH\cdot \xrightarrow{\text{irradiation}} S\cdot + 2NH_3 + CO_2 \quad (4)$$

$$Zn^+ + S\cdot + e^-_{aq} \rightarrow ZnS \quad (5)$$

Here, the sulfur radicals (S·), not S^{2-} ions, could gradually be liberated from thiourea or CS_2 under γ-irradiation and could then react slowly with the lower-valence zinc ions (Zn^+) formed by reduction of Zn^{2+} by solvated electrons (eq 2). The formation of ZnS nanocrystallites occurs in a homogeneous system, and the slow liberation of sulfur radicals is favorable for the oriented growth of nanowires. Moreover, ZnS atomic clusters are formed first, and then the ZnS nanowires start to grow when the ZnS atomic clusters are in an excess saturation state. This formation mechanism is similar to that of silicon nanorods.[6] In addition, the aqueous channels of the inverted hexagonal liquid crystal template also play an important role in defining the growth of the ZnS nanowires. During our experiments, we did not find the appearance of zinc metal in the products, except for a small amount of elemental sulfur. Compared to the formation of the ZnS nanowires, when only the zinc salt solution is added to the inverted hexagonal liquid crystal system and irradiated by γ-ray for 6 h, no metallic zinc forms in this system. When only the sulfur source of CS_2 or thiourea is added to the inverted hexagonal liquid crystal system, a small amount of elemental sulfur forms. This suggests that a small amount of elemental sulfur probably forms in the process of formation of the ZnS nanowires but that the elemental sulfur can be washed with CS_2 solution and have no influence upon the characterization of the ZnS nanowires.

The composition of final product was determined by XRD (Figure 3), which shows the presence of broad peaks corresponding to the zinc blende crystal structure. The three strong diffraction peaks correspond to the 111, 220, and 311 planes of the cubic crystalline ZnS (JCPDS No. 5-566). The average size is 5.6 nm, as estimated from the Debye−Scherrer formula, which is nearly consistent with the size of the ZnS nanowires determined by the TEM observations.

Figure 4 shows the XPS spectra of the product, including (a) the survey spectra, (b) S 2p, (c) Zn 2p3, and (d) Zn LMM. The binding energy values are 163.3 eV for S 2p and 1022.7 eV for Zn 2p3, and the kinetic energy for Zn LMM is 988.7 eV. These results are consistent with the values reported by Wagner.[32] The ratio of integral area for S 2p to Zn 2p3 is about 1:1.085, and the amount of impurities such as CO_2, H_2O, and O_2 adsorbed on the surface of the ZnS nanomaterials is small, as can be seen from the survey spectrum of the sample.

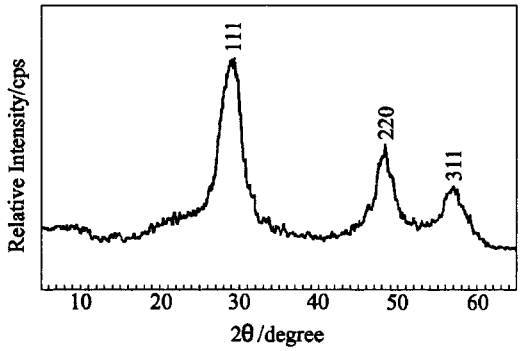

Figure 3. XRD pattern of ZnS nanowires after removal of the inverted hexagonal liquid crystal template and washing with a 50:50 vol % solution of diethyl ether/ethanol via sonication.

Figure 5 displays the TEM images of the ZnS nanowires. The regularly shaped ZnS bundles prepared in the inverted hexagonal liquid crystal template are shown in Figure 5a. The average size of the ZnS nanowires is 20 × 1200 nm. After removal of the amphiphiles via a 50:50 vol % solution of diethyl ether/ethanol, the structure of the ZnS bundles is also regularly shaped and the size of sample has changed little (Figure 5b). Figure 5c shows one magnified part of a bundle that contains seven or more parallel ZnS nanowires (indicated by arrows), which duplicates the characteristics of the inverted hexagonal liquid crystal phase. The diameter of each wire in a bundle is ca. 5 nm, which is nearly consistent with the diameter of the hydrophilic cavities (4.6 nm). This also suggests that the hexagonal mesophase template is suitable for synthesis of ordered nanowires. Figure 5d shows an electronic diffraction (ED) pattern of a selected area within a linear segment of a bundle of ZnS nanowires and the single-crystal pattern with the 110 direction for cubic ZnS. Two typical diffraction spots are indexed as the 111 and 220 planes, which is consistent with the diffraction peaks indexed in the XRD pattern (Figure 3). The atomic ratio of Zn to S in the product is 1:1.05, as measured by the EDX analysis.

(31) Qiao, Z.; Xie, Y.; Qian, Y.; Zhu. Y. *Mater. Chem. Phys.* **2000**, *62*, 88.

(32) Wagner, C. D.; Riggs, W. W.; Davis, L. E.; Moulder, J. F.; Muilenberg, G. E. *Handbook of X-ray Photoelectron Spectroscopy*; Physical Electronics Division, Perkin-Elmer Corporation: Wellesley, MA, 1979.

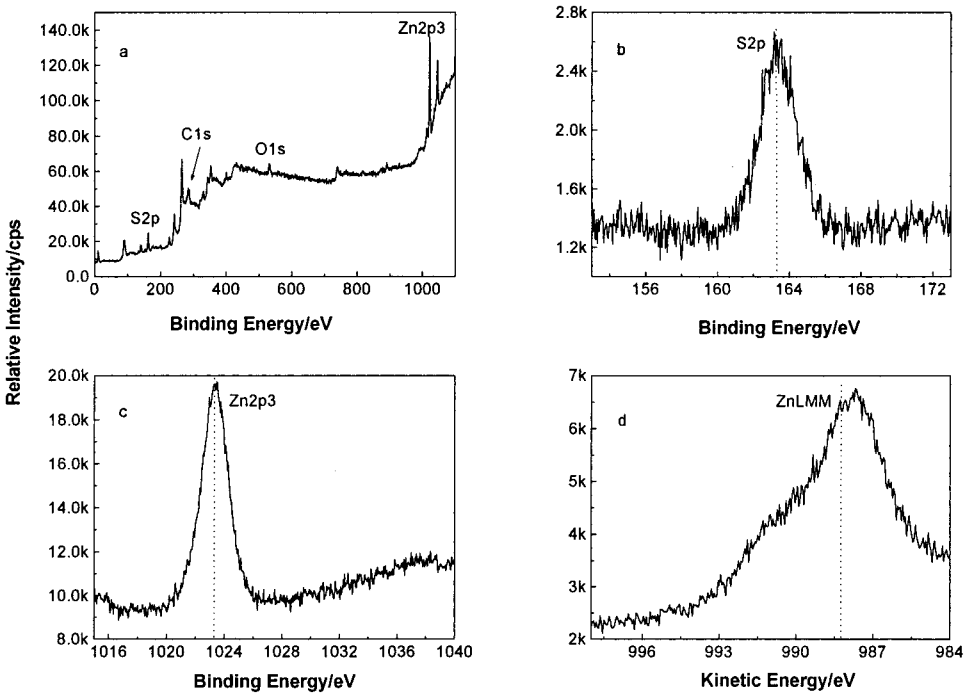

Figure 4. XPS spectra of ZnS nanowires: (a) survey spectrum, (b) S 2p, (c) Zn 2p3, and (d) Zn LMM.

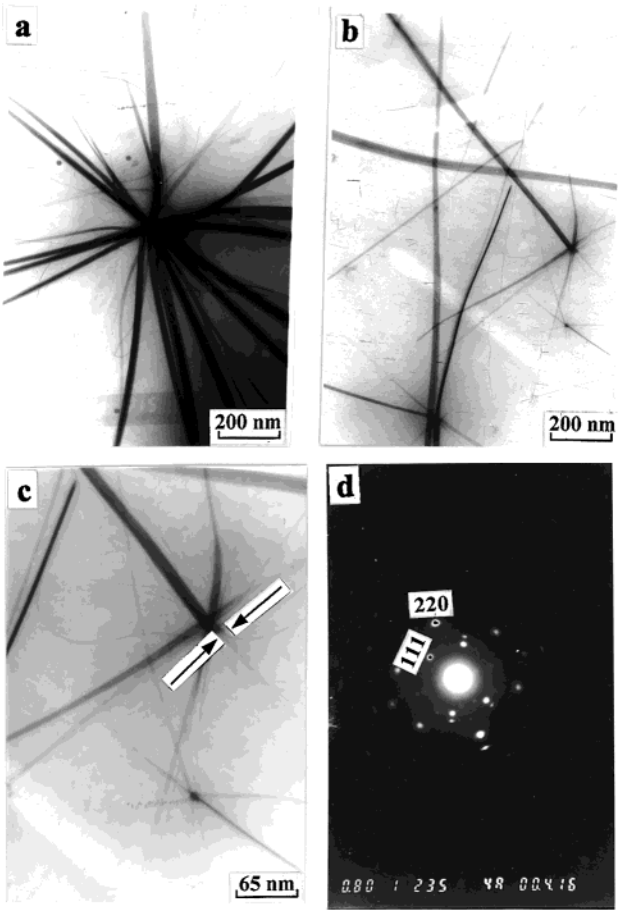

Figure 5. (a) TEM image of ZnS nanowires before the liquid crystal (LC) template is removed, (b) TEM image of ZnS nanowires after the LC template is removed, (c) one magnified part of a ZnS bundle composed of seven or more nanowires, and (d) ED pattern of ZnS nanowires after the LC template is removed.

Figure 6 shows the optical absorption and photoluminescence spectra of the ZnS nanowires. An absorption peak appears at ~326 nm (solid line) and has a modest blue-shift (~19 nm) compared to the corresponding peak for bulk ZnS (345 nm).[33] This shift can be attributed to quantum size effects of the ZnS nanocrystallites obtained from the hexagonal mesophase. The PL spectrum of the ZnS (dotted line) shows a broad emission band centered at ~366 nm and a weak shoulder peak at ~330 nm (λ_{ex} = 300 nm). A marked blue shift (~74 nm) of the emission band position relative to that of the bulk ZnS (440−500 nm) is observed, which might be due to the quantum size effects of the ZnS nanocrystals. Furthermore, it is worth mentioning that other studies[34] have detected two blue emissions centered at 428 and 418 nm in colloidal suspensions of ZnS, which are assigned to a sulfur vacancy and interstitial sulfur lattice defects, respectively.[34] Early interpretations have attributed the ZnS emission to a cation vacancy whose nearest surround-

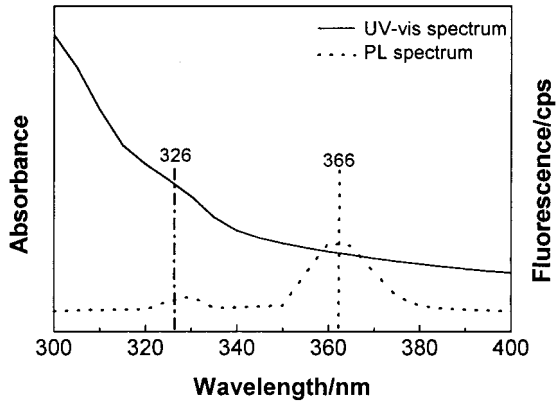

Figure 6. UV−visible and photoluminescence spectra (λ_{ex} = 300 nm) of ZnS nanowires formed in the inverted hexagonal liquid crystal phase.

(33) *Introduction to Solid State Physics*; Kittel, C., Ed.; Wiley: New York, 1986; Chapter 8.
(34) Becker, W. G.; Bard, A. J. *J. Phys. Chem.* **1983**, *87*, 4888.

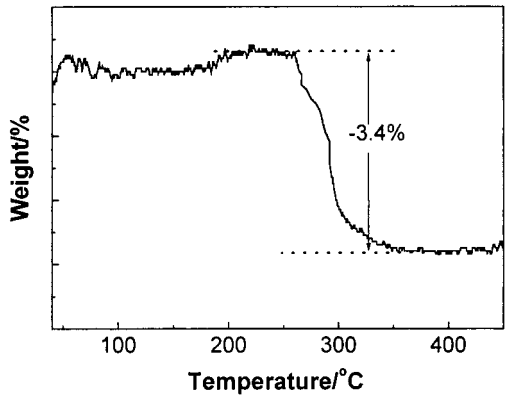

Figure 7. TGA of ZnS nanowires after removal of the liquid crystal phase by washing with a 50:50 vol % solution of diethyl ether/ethanol and sonication.

ings have lost one electron.[35] The ZnS emission band centered at 420 nm can be assigned to emission from the recombination of electrons and holes in trapped surface states located in the "forbidden" region of the band gap.[36] The observed emission band from the suspensions of ZnS in our experiments can be assigned to a sulfur vacancy and interstitial sulfur lattice defects, as in the literature.[34]

The weight loss of amphiphiles bound with ZnS was determined and shown in Figure 7. From the TGA curve, the weight loss of ZnS is about 3.4% from 260 to 340 °C. After the sample is heated over 340 °C, the sample weight does not change again. This shows that only a small amount of organic molecules is bound to the ZnS nanowires after they are washed.

(35) Kroger, F. A.; Vink, H. J. *J. Chem. Phys.* **1954**, *22*, 250.
(36) Cizeron, J.; Pileni, M. P. *J. Phys. Chem.* **1997**, *101*, 8887.

4. Conclusions

Ordered ZnS nanowires with the diameter of ca. 5 nm were obtained in a hexagonal liquid crystal template under γ-irradiation. Here, the γ-irradiation plays an important role in the formation of ZnS nanowires using thiourea or CS_2 as the sulfur source. The new approach avoids the use of toxic H_2S gas. The formation occurs homogeneously and simultaneously in the inverted hexagonal mesophase. Most importantly, several close-packed nanowires aggregate to form bundles with diameters ranging from 10 to 30 nm, which duplicate the hexagonal structure of close-packed inverted micelles formed by amphiphiles. The composition and morphology of ZnS were determined by XRD, XPS, TEM, and EDX techniques. The UV−vis absorption maximum of ZnS nanowires is 326 nm, with a modest blue-shift relative to that of bulk ZnS (345 nm) due to quantum size effects. The emission wavelength maximum in the photoluminescence (PL) spectrum of the ZnS nanowires is 366 nm, with a weak shoulder peak at 330 nm (λ_{ex} = 300 nm), which is markedly blue-shifted relative to the corresponding peak of bulk ZnS (440−500 nm). This peak is assigned to a sulfur vacancy and interstitial sulfur lattice defects. The amount of amphiphiles bound to the ZnS nanowires was about 3.4 wt %, as measured by TGA techniques. The SISF technique assisted by γ-irradiation can be applied to the synthesis of a wide variety of technologically important one-dimensional semiconductor nanomaterials.

Acknowledgment. Financial support from the Chinese National Foundation of Natural Science Research and the China Ministry of Education is gratefully acknowledged.

CM0006143